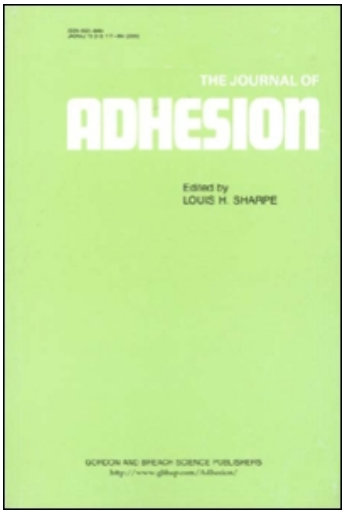

The Journal of Adhesion
Publication details, including instructions for authors and subscription information:
http://www.informaworld.com/smpp/title~content=t713453635

Effect of Adhesive Thickness on Joint Strength: A Molecular Dynamics Perspective

A. Adnan[a]; C. T. Sun[a]
[a] School of Aeronautics and Astronautics, Purdue University, West Lafayette, IN, USA

To cite this Article Adnan, A. and Sun, C. T.(2008) 'Effect of Adhesive Thickness on Joint Strength: A Molecular Dynamics Perspective', The Journal of Adhesion, 84: 5, 401 — 420
To link to this Article: DOI: 10.1080/00218460802089239
URL: http://dx.doi.org/10.1080/00218460802089239

The Journal of Adhesion, 84:401–420, 2008

ISSN: 0021-8464 print/1545-5823 online
DOI: 10.1080/00218460802089239

Taylor & Francis
Taylor & Francis Group

Effect of Adhesive Thickness on Joint Strength: A Molecular Dynamics Perspective

A. Adnan and C. T. Sun
School of Aeronautics and Astronautics, Purdue University, West Lafayette, IN, USA

Recent studies suggest that adhesion in thin joints depends on several factors including temperature, interface toughness, strain rate, surface roughness of adherends, bondline thickness of adhesives, and many others. Influence of thickness on joint properties is surprising but experimentally well documented without reasonable explanations. In this study, we attempt to address the mechanical behavior of polymer adhesives by molecular dynamics (MD) simulation. We show that interfacial strength of the joints in tensile, shear, or combined loading significantly depends on the coupling strength between adhesives and adherends. Failure of joints is always at the interface when coupling strength is weaker. With stronger interfaces, cohesive failure occurs by cavitation or by bulk shear depending on the loading condition. When joints are loaded in tension, it requires an exceedingly stronger interface to realize pure shear failure, otherwise failure is through interface slip. Under a mixed mode condition, interface slip is difficult to avoid. As long as failure is not at the interface alone, the yield strength of joints improves significantly with the reduction of thickness. Increase in bulk density and change in polymer configurations with the reduction of adhesive thickness are believed to be the two key factors in improving mechanical behavior of adhesives.

Keywords: Adhesive thickness; Failure; Interface strength; Molecular dynamics; Shear; Tensile

1. INTRODUCTION

The mechanical behavior of adhesive joints is of great technological importance due to their widespread applications in aerospace, automotive, sporting goods, household, and packaging industries [1].

Received 17 November 2008; in final form 7 February 2008.

Address correspondence to C. T. Sun, School of Aeronautics and Astronautics, Purdue University, 701 West Stadium Avenue, Neil Armstrong Hall of Engineering, West Lafayette, IN 47907-2023, USA. E-mail: sun@purdue.edu

In recent years, very thin layers of adhesives have been extensively used in the micro/nano-electromechanical (MEMS/NEMS) or micro-opto-electromechanical (MOEMS) systems to fabricate micro/nano devices including micro-actuators, pressure sensors, etc. [2]. The behavior of joints at yield is usually characterized experimentally by tensile or shear tests, whereas the resistance to fracture is portrayed by end-notch flexure (ENF) or double-cantilever-beam (DCB) type fracture tests [1].

In general, failure of polymer-based adhesive joints can be classified into four categories [1,3,4]: (a) cavitation or shear failure in the bulk polymer (cohesive failure), (b) debonding at the polymer-adherend interface (adhesive failure), (c) combined adhesive-cohesive failure, or (d) adherend failure. Cohesive failure occurs when the cohesive strength of polymer is lower than the interface strength, whereas, adhesive failure takes place when the interface is weaker. For a joint where the cohesive strength and interface strength are of the same order, its failure mode may then turn into a combined adhesive-cohesive failure. In real applications, adherend materials are usually two to three orders of magnitude stronger than adhesives, hence, an adherend failure may only occur by premature failure in the adherends due to flaw or impurity induced local stress concentrations.

It is observed in joints with relatively soft polymer adhesives that the thickness of adhesives significantly influences the mechanical behavior of joints, particularly when the bondline thickness becomes smaller [5–11]. For example, the failure loads of lap joints in lap-shear tests are monotonically increased with the reduction of adhesive thickness [5,6]. In these experiments, the thinnest adhesive tested was in the range of 0.1 to 0.2 mm. Dramatic change in the failure load was also observed in joints with thickness below 0.1 mm. Objois *et al*. [7] found that the failure load was continuously increased as the adhesive thickness was decreased from 1 to 0.1 mm. The load was then suddenly decreased when thickness was reduced to 0.05 mm. The authors argued that that the non-uniform stress distribution in the thinnest adhesive caused local stress concentration and subsequently led to premature failure of the joint.

Significant effect of bondline thickness on fracture toughness of adhesives has also been observed [8–11], and the results are quite interesting. It appears from most of these experiments that the critical fracture energy (G_{IC}) of adhesive joints attains a maximum value at some bondline thickness t_c. The value of G_{IC} then gradually drops and becomes insensitive to thickness for thicker adhesives. Surprisingly,

the magnitude of G_{IC} also decreases with thicknesses smaller than t_c. In these experiments, the value of t_c was found to be on the order of ~ 0.5 mm. A number of researchers attempted to explain this unusual phenomenon from different perspectives. For example, Bascom *et al*. [8] suggested that the variation of the G_{IC} with bondline thickness depends on the plastic zone size ahead of the crack tip, and the G_{IC} reaches the maximum value when bond thickness becomes equal to the plastic zone diameter. Kinloch and Shaw [9] explained that the G_{IC} depends on the area of the plastic zone, and that the constraining effects from the two adherends control the plastic zone size. With thickness smaller than the t_c, the plastic zone cannot fully form due to the confinement by the hard substrates. On the other hand, when thickness becomes larger than t_c, the substrates impose less constraints on the adhesive, and, thus, lessens energy dissipation. Lee *et al*. [10] pointed out that the presence of toughening agents (rubber particles) in the structural adhesive might have caused changes in the crack propagation direction as the bondline thickness decreases. Diversion of crack propagation then led to the variation in critical fracture energy. The most interesting trend on this issue was reported by Chai [11] who successfully fabricated adhesives as thin as 5 μm and observed that the critical fracture energy attained the maximum value at thickness around 0.2 mm. With thickness smaller or larger than this critical value, the G_{IC} decreased. Surprisingly, the trend was reversed for thickness below 0.033 mm and G_{IC} started to increase with the decrease in thickness. The author pointed out that this distinctive trend is associated with the shift of failure from the load center to the metal-matrix interface zones.

Several observations can be made from the study of the thickness effect on the failure and fracture of adhesive joints when thickness reduces to the micrometer scale or below. Maintaining uniform thickness as well as uniform properties of adhesives in thinner joints is extremely challenging. A slight variation in the configuration might cause severe effects on the test data. Apart from the fabrication difficulties, various intermolecular and surface forces might be involved in the adhesives when thickness reduces to sub-micrometer scale [1]. Significant changes in the polymers' structures may also occur near the substrate walls including layering of polymer chains, increased segmental densities, etc. [12]. In order to achieve a microscopic understanding of deformation and failure of adhesives and their relation to the bondline thickness, atomistic simulation of adhesive joints could be a helpful tool.

In this paper, we present a series of molecular dynamics (MD) simulation results that include the effect of thickness on mechanical

behavior of glassy polymer adhesive joints. In our model, we have chosen the range of thicknesses at the nanoscale dimension. The model allows us to investigate various loading modes for adhesives with different thicknesses as well as with different interface conditions. We organize the paper in the following manner. The next section provides the technical details of the simulations. In the subsequent section, we describe the effect of thickness and interface strength on the stress-strain response and failure behavior of adhesives. We have simulated tensile, shear, and combined loading for all adhesive models and discussed the failure modes.

2. MOLECULAR MODELS FOR ADHESIVE JOINTS

Molecular models of the adhesives are developed by confining polyethylene (PE) chains between metal walls, as shown schematically in Fig. 1(a). The dashed box in Fig. 1(a) corresponds to the unit cell that is simulated by MD and shown in Fig. 1(b). The finite thickness of the unit cell was maintained by applying periodic boundary

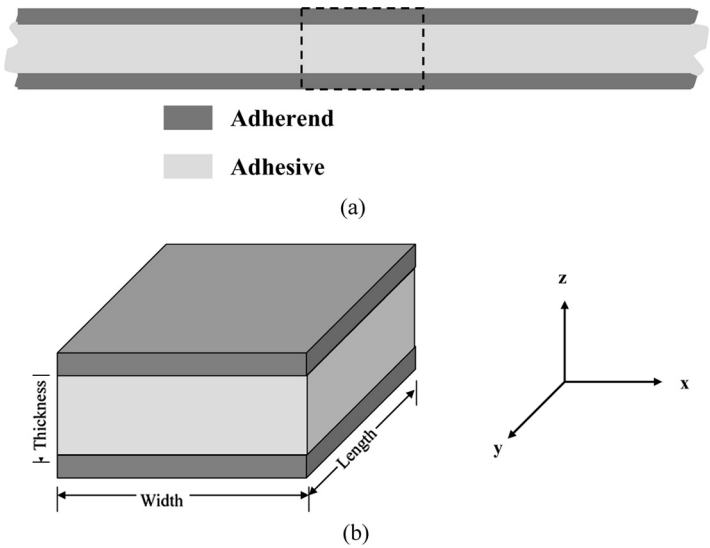

FIGURE 1 (a) Schematic diagram of an adhesive joint. The structure infinitely spans along x-and y-direction with finite thickness along z-direction. (b) Unit cell used for MD simulation. Periodic condition is imposed along the width and length directions. No periodicity is prescribed along height direction.

conditions along the x-and y-directions only. For this study, three models of adhesive joints are developed with nominal thickness of 2, 4, and 5 nm, respectively. For consistency, the width and length of the adhesive joints, dimensions of adherend materials, the type of polymer adhesive and its initial density, and the simulation temperature were kept constant. Here the PE adhesives are represented by united atom (UA) $-CH_2-$ units and their initial configurations are constructed by randomly generating PE chain(s) with a temperature-dependent, self-avoiding random walk (SARW) algorithm for an initial density of $0.85\,gm/cm^3$ [13]. The chosen density corresponds to the typical linear amorphous polyethylene [12,14,15].

In the simulation, all PE chains are described by appropriate potential functions that include 2-body, 3-body and 4-body potentials between $-CH_2-$ units [16]. Specifically, the bond length between $-CH_2-$ units of the PE chain is constrained to 1.53 Å *via* the SHAKE algorithm [13]. The angle bending energy or the three-body term are modeled with a harmonic valence-angle potential of the form

$$U_{\text{angle}}(\theta) = \frac{1}{2}k_\theta[\theta - \theta_0]^2, \tag{1}$$

where $U_{\text{angle}}(\theta)$ is the angle-bending potential energy, θ is the angle between two bonds, $k_\theta = 124.2\,\text{kcal/mol}$, and $\theta_0 = 112.0$. The functional form of the four-body term or the dihedral potential energy is prescribed by

$$U_{\text{dihedral}}(\phi) = \frac{A_1}{2}[1 + \cos(\phi)] + \frac{A_2}{2}[1 - \cos(2\phi)] + \frac{A_3}{2}[1 + \cos(3\phi)]. \tag{2}$$

Here $U_{\text{dihedral}}(\phi)$ is the dihedral energy, ϕ is the dihedral angle around the CH_2–CH_2 bond, and $A_1 = 1.411$, $A_2 = -0.271$, and $A_3 = 3.145\,\text{kcal/mol}$.

The non-bonded van der Waals (VDW) interactions within or between PE chains are modeled with the Lennard-Jones (LJ) potential [13],

$$U_{LJ}(r) = 4u\left[\left(\frac{a}{r}\right)^{12} - \left(\frac{a}{r}\right)^{6}\right], \tag{3}$$

where U_{LJ}(r) is the potential energy between a pair of atoms, r is the separation distance between them, u is the potential well depth, and a is the VDW separation distance. For the interaction between the $-CH_2-$ units, the potential was parameterized with $u = 0.118\,\text{kcal/mol}$ and $a = 3.905$Å.

The polymer adheres to the metal walls that consist of several layers of a Face Centered Cubic (100) crystal. It is known that adherends are usually two to three orders of magnitude stiffer than adhesives. For computational convenience, we assumed that adherend walls are non-deformable or "rigid". The rigid configuration is achieved by expressing the adherend atoms as a set of "Frozen" atoms during the MD simulation [17,18]. The interactions between the PE adhesive and rigid walls are modeled and evaluated by the same LJ potential shown in Eq. (3) but with u and a replaced by $u^0_{wa} = 0.1403\,\text{kcal/mol}$ and $a^0_{wa} = 3.11\text{Å}$. Here, u^0_{wa} and a^0_{wa} are obtained by the mixing rule,

$$\begin{aligned} u^0_{wa} &= \sqrt{u^0_{wall} u^0_{PE}} \\ a^0_{wa} &= \frac{a^0_{wall} + a^0_{PE}}{2}. \end{aligned} \tag{4}$$

In Eq. (4), the subscripts "wall" and "PE" represent LJ parameters for the wall atoms (adherends) and the PE molecules (adhesive), respectively. In order to address various interface conditions representing incompatible/poor and enhanced/treated interfaces, the "PE-Wall" interaction strength is modified by varying the energy scale, u^0_{wa}, between 0.25 u^0_{wa} to 4.0 u^0_{wa}. Here, the higher value of u^0_{wa} implies a stronger interface.

3. MOLECULAR SIMULATION OF DEFORMATION AND FAILURE OF JOINTS

The MD simulations were performed using DL-POLY (version 2.15) simulation package developed by Daresbury Laboratory (Daresbury, Warrington, Cheshire, UK) [19]. All simulations were carried out at 100K with 0.5 fs time steps. The stress-strain relation was obtained by performing simulations in two major steps. In the first step, the equilibrium state of the molecular model was obtained. In the next step, the model was appropriately subjected to incremental strain fields with subsequent equilibration.

3.1. Equilibrium State

In this step, relaxed states of all adhesive models are obtained. From the MD point of view, attainment of such a state requires fulfillment of two major criteria, *i.e.*, to achieve the energy stabilized state at a prescribed temperature, and to obtain the minimum initial stress state for the unit cell. In the current study, the molecular model for polyethylene adhesives was first created in the molten state. Then it was

gradually condensed to 100K by using NPT (constant number of atoms, pressure, and temperature) ensembles for 200 ps. The temperature and pressure were controlled by the Nosé-Hoover (NH) [13] thermostat and barostat (with equal thermostat and barostat time constant of 1 ps). The system was further equilibrated by NVT (constant number of atoms, volume, and temperature) for 10 ps. As before, the constant temperature was maintained by the NH thermostat. At the end of these steps, all molecular models were believed to be completely relaxed at 100K with the minimum initial stress.

3.2. Loading

Each joint was loaded with pure tensile, pure shear, and combined tensile and shear. The corresponding stress-strain curves were generated *via* MD simulation by uniformly deforming the unit cells along the desired directions. The entire loading process was carried out at a constant temperature (NVT) simulation with the temperature controlled by NH (thermostat time constant = 1 ps).

In order to apply the desired load, the two rigid walls were displaced simultaneously with the strain increment of 0.05% as shown in Fig. 2. After each strain increment, the whole system was equilibrated for 2000 time steps (1 ps), followed by data sampling and averaging for the next 1000 time steps. It was ensured that the length of the equilibration periods was large enough to attain equilibrium in the whole system before measurements were recorded and the next increment was applied. The recorded data at the end of these incremental steps generated the desired stress-strain curve.

The response of the adhesive joint with the applied strain field was monitored by measuring various stress fields (σ_{ij}). The definition of stress, however, is different from what is prescribed at the continuum level. At the atomic level, stress can be defined in the form of "virial stress" as

$$\sigma_{ij} = -\frac{1}{V}\sum_{\alpha}\left(M^{\alpha}v_i^{\alpha}v_j^{\alpha} + \frac{1}{2}\sum_{\beta\neq\alpha}F_i^{\alpha\beta}r_j^{\alpha\beta}\right), \tag{5}$$

where V is the characteristic volume of the MD unit cell with $V = \sum \alpha V^{\alpha}; V^{\alpha}$ is the atomic volume of atom α, v_i^{α} is the i-component of the velocity of atom α, v_j^{α} is the j-component of the velocity of atom α, $F_i^{\alpha\beta}$ is the i-component of the force between atoms α and β, and $r_j^{\alpha\beta}$ is the j-component of the separation distance between atoms α and β. It can be seen that Eq. (5) represents average atomic stresses for the volume of the unit cell. Here, the first term is associated with the

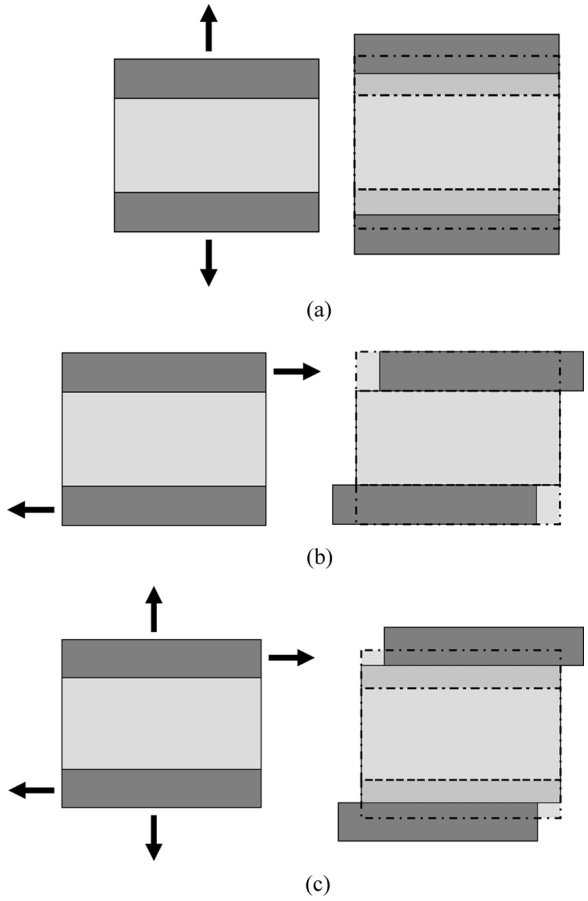

FIGURE 2 Schematic diagram of deformed (Right) and un-deformed (Left) configuration of the unit cell showing (a) tensile, (b) shear, and (c) combined tension-shear loading. Dashed lines in right figures represent undeformed configurations.

contribution from kinetic energy due to thermal vibration and the second term is related to change in potential energy due to applied deformation. The negative sign is used to express tensile stress as a positive quantity (in MD, compression is generally expressed as positive). In our simulation, we estimated the total volume, V, as

$$V = L_x L_y t_0, \tag{6}$$

in which L_x and L_y are the lengths of the unit cell along the x- and y-directions, respectively, and t_0 is the thickness of the adhesive.

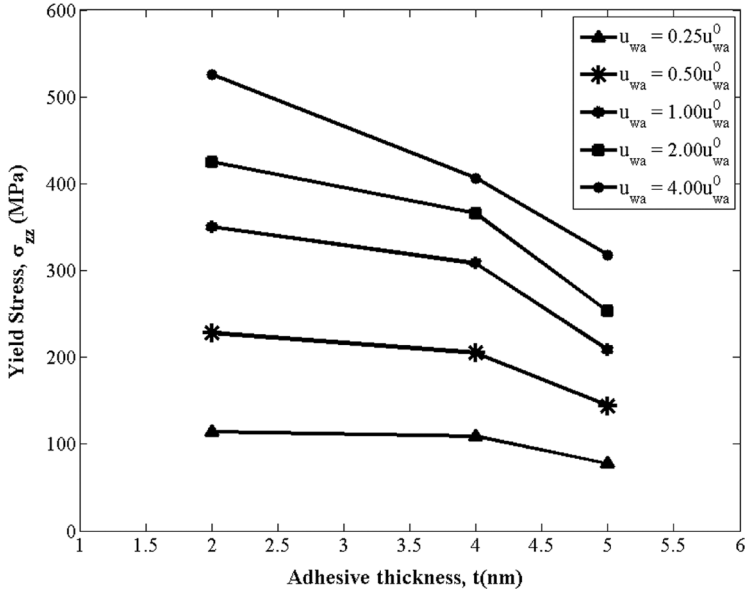

FIGURE 3 Effect of thickness and interface strength on the maximum tensile stress.

4. RESULTS AND DISCUSSION

In order to obtain unidirectional tension and shear, the adherend walls were moved vertically (z-direction) and horizontally (x-direction) in the opposite sense, respectively. The two walls were moved simultaneously and equally in the horizontal and vertical directions for combined loading. We then obtained the stress-strain relations for each joint, recorded the corresponding maximum stresses, and then plotted against adhesive thickness. The results are shown in Figs. 3–5.

4.1. Effect of Coupling Strength u_{wa} on Failure Mode

It is evident from Figs. 3–5 that the peak stress, also considered here as the yield stress, are governed by the coupling strength, u_{wa}, between the adherend wall and the polymer. In Figs. 6–8, the atomistic deformations during various loadings are illustrated with snapshots taken at some post-yield strains. It can be observed from Fig. 6 that all joints loaded in tension fail at the interface when $u_{wa} < 1.0u^0_{wa}$. Higher values of u_{wa} lead to the cohesive failure through cavitations inside the polymer adhesives. It is evident from Fig. 4 that

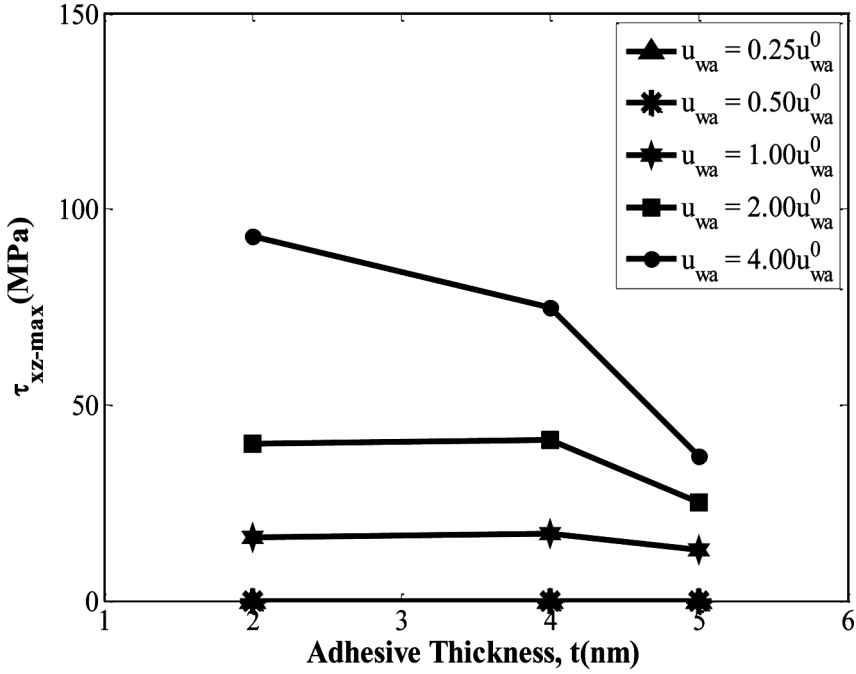

FIGURE 4 Effect of thickness and interface strength on the maximum shear stress.

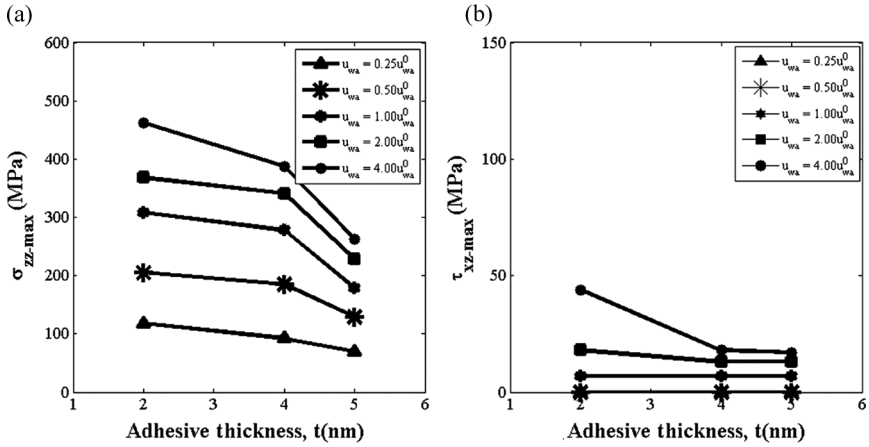

FIGURE 5 Effect of thickness and interface strength on (a) maximum tensile stresses and (b) maximum shear stress, under combined tensile-shear loading.

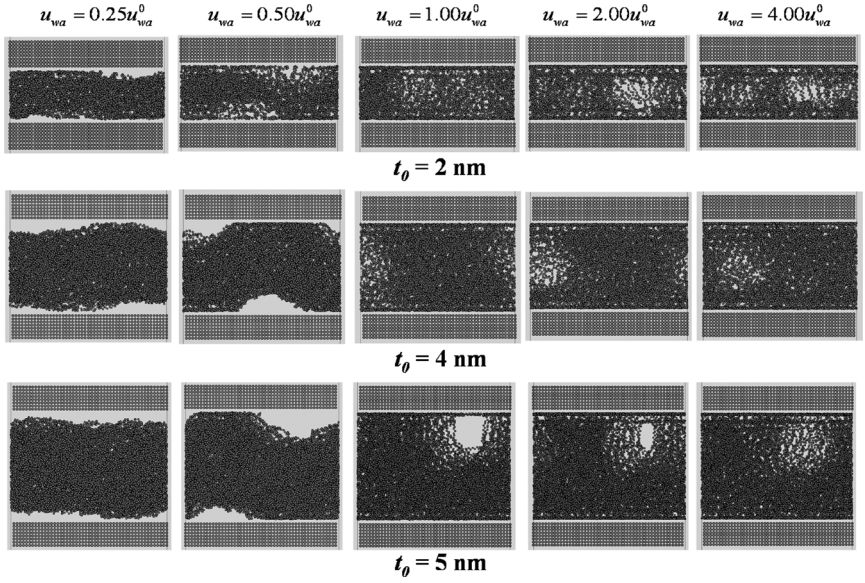

FIGURE 6 Molecular Simulation snapshots of different adhesives under tensile loading at 20% strain. Pictures from left to right correspond to changing from weaker to stronger interface. Note that 20% strain implies post-yield deformation of joints.

joints bear no load when $u_{wa} \leq 1.0u^0_{wa}$ indicating the possibility of interface failures. It is, however, not confirmed that joints failed in bulk shear for a value of $u_{wa} > 1.0u^0_{wa}$. MD snapshots, as shown in Fig. 7, also do not give any clear indication.

In order to visualize the response of molecular chains when two walls are displaced in shear, we mapped the displacement of some $-CH_2-$ united atoms in a slab that was sectioned from an unloaded unit cell (Fig. 1). The width of the slab spans ± 1.6Å away from the z-axis. Its other dimensions extend to the full length of the original unit cell. Note that the origin of the axes is at the center of the unit cell, and the length and width of the unit cell are ~ 42Å, whereas the height is ~ 30Å plus the thickness of the adhesive. First, the group of atoms within the slab is identified in the unloaded unit cell, and their relative positions are then monitored at different strain states and plotted. In Fig. 9, we only illustrate the results for a 4 nm thick joint because we found similar behavior for other joints. It is noted that the width of the slab is chosen such that it contains only one layer of wall atoms across the thickness direction. Note that at 0.0% strain

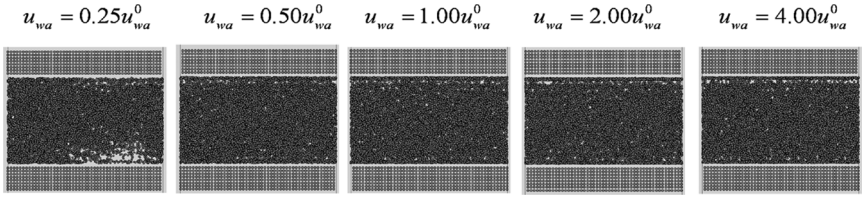

FIGURE 7 Molecular simulation snapshots of 4 nm thick adhesives under pure shear loading at 35% strain. View of snapshots for other joints appears similar.

all atoms are located inside the rectangular slab of width 3.2Å. It can be seen from Figs. 9(a) and (b) that almost all polymer atoms are detached from the wall atoms shortly after the joint is loaded. Such deformation corresponds to $u_{wa} \leq 1.0u^0_{wa}$ and clearly portrays that interfacial slip occurs in the joint as soon as the walls are displaced. Figs. 9(c) and (d) show the displacement of the polymer molecules corresponding to $u_{wa} > 1.0u^0_{wa}$. It appears that the polymer chains are

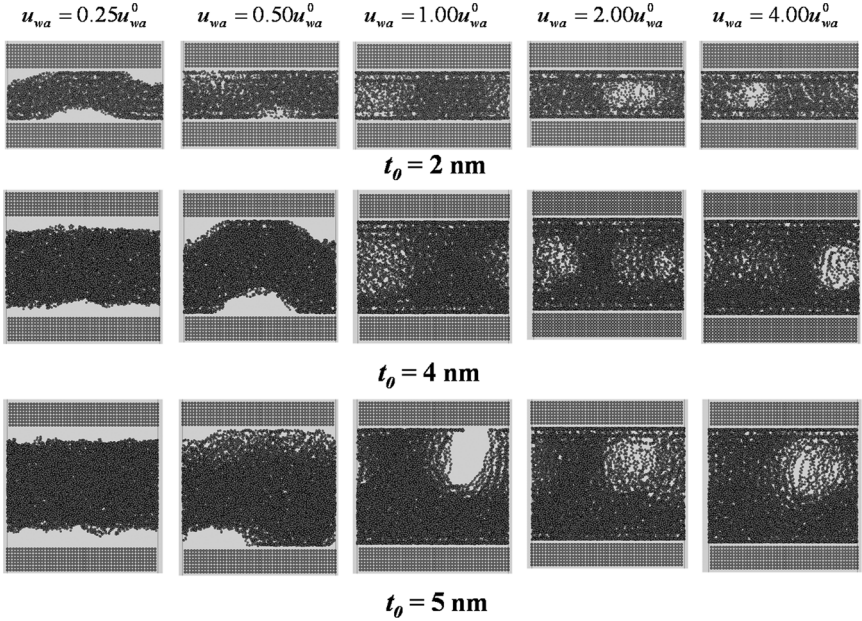

FIGURE 8 Molecular simulation snapshots of different adhesives under combined tensile and shear loading at 35% strain.

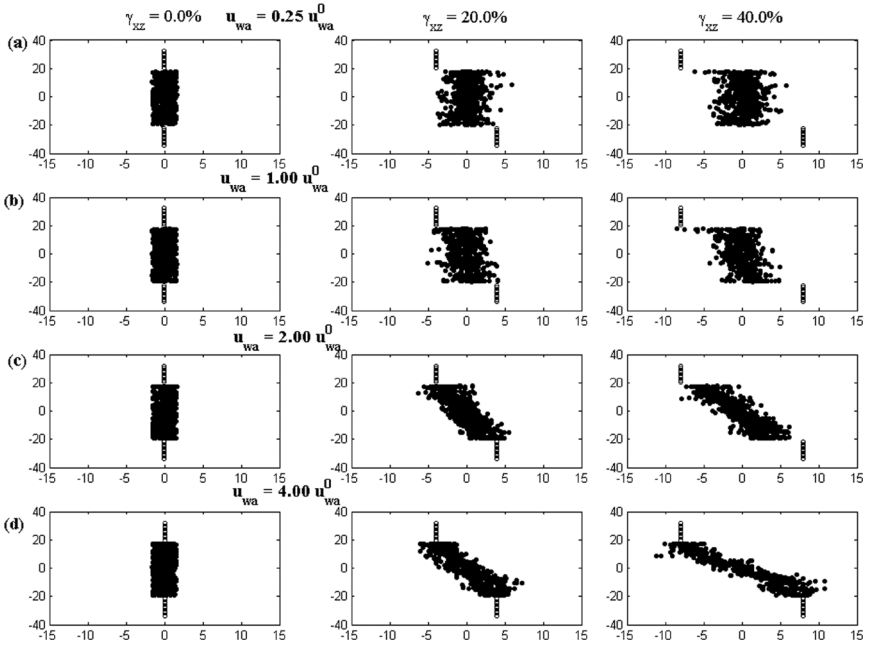

FIGURE 9 Mapping of selected −CH2− units under shear loading. Atoms were selected from an imaginary slab parallel to the z plane that was sectioned from the middle of a unit cell. Plots shown for deformation of the 4 nm thick adhesive. Figures (a) thru (d) correspond to wall-adhesive coupling strength, u_{wa} from 0.25 u^0_{wa} to 4.0 u^0_{wa}. In each case, atoms were mapped at an interval of 20% strain state until the end of simulation (40% strain). Open and closed circles represent the wall atoms and PE united atoms, respectively.

deformed and stretched in shear up to $\gamma_{xz} < 20\%$. It is, however, noticed from Fig. 9(c) that failure actually occurs *via* interfacial slip at $\gamma_{xz} \geq 20\%$. For $u_{wa} = 4.0u^0_{wa}$, we found no slip up to 40% strain.

TABLE 1 Bulk Polymer Density in Various Joints

	Density, ρ (gm/cm^3)		
Coupling Strength	2 nm	4 nm	5 nm
0.25 u^0_{wa}	0.9622	0.9674	0.9302
0.50 u^0_{wa}	0.9798	0.9812	0.9407
1.00 u^0_{wa}	1.0009	0.9924	0.9503
2.00 u^0_{wa}	1.0342	1.0111	0.9653
4.00 u^0_{wa}	1.0682	1.0304	0.9836

It may be concluded from Fig. 9 that, as long as the adherends are atomically flat, the interfacial slip may not be avoided even with stronger interfaces. To ensure pure bulk shear, some means of surface roughness [3] or chemical functionalization [20] appears to be necessary to produce mechanical or chemical interlocking.

When adhesives are loaded simultaneously in tension and shear, all joints failed at the interface when $u_{wa} \leq 1.0u_{wa}^0$. With $u_{wa} > 1.0u_{wa}^0$, the mode of failure is of the mixed adhesive-cohesive type, except for the 2 nm adhesive which failed cohesively. This happens because the interfacial slip is unavoidable under shear with the choice of u_{wa} studied here even though the tensile failure is caused by cavitation.

4.2 Effect of u_{wa} on the Joint Strength

It appears from Figs. 3–5 that for any joints, the maximum tensile or shear stress is directly related to the interface coupling strength, u_{wa}, regardless of whether the failure mode is cohesive or adhesive. This is somewhat surprising because, in principle, the magnitude of u_{wa} should not affect the overall cohesive strength of the polymer; and, hence, all stress-strain curves should collapse on the same plot [3]. Basu and Kulmi [4], however, found that the magnitude of the coupling strength changes the mode of failure from adhesive-cohesive to pure cohesive. This was evidenced by $\sim$40% increase in joint strength with the significant increase in coupling strength. They, however, did not find any effect of coupling strength on initial modulus of joint. They also demonstrated that once pure cohesive strength was guaranteed, the yield strength of the joint also became insensitive to coupling strength.

The reason why we observe higher stresses with increased u_{wa} can be understood from the effect of u_{wa} on polymer bulk density (see Table 1). It is evident that, as u_{wa} increases, the overall density of the polymer also increases considerably. For example, the bulk density of the thinnest adhesive increased from 0.9622 to 1.0682 gm/cm^3 as the coupling strength increased from 0.25 u_{wa}^0 to 4.0 u_{wa}^0. This increased density of the polymer, which rises monotonically as u_{wa}^0 increases, is a result of densely packed monomers near the walls in the form of several aligned layers. Such layers are formed due to non-bonded VDW interaction between polymer and wall atoms. The relative density of this zone depends on the interface strength while the effective range of VDW potential energy controls its depth. With potentials described by Eq. (3), the span of the denser zone is found to be $\sim 2\, a_0$(a_0 = equilibrium separation distance between VDW atom

pairs) which translates to ~ 0.8 nm for the particular adherend-adhesive system studied here. Since mechanical properties are directly related to the density of material, this possibly is why the cohesive strength of adhesives increases with increase in coupling strength.

If we consider the denser zone close to the wall as the "effective VDW zone," henceforth referred to as EVZ in the remainder of the text, then the proportion of this EVZ compared with adhesive volume is higher for the thinner adhesives. As can be seen from Table 1, the 2 nm thick adhesive is denser than the other adhesives because it contains more EVZin terms of volume fraction. It is also apparent that for 2 nm thick adhesives, the entire thickness is almost within the PE-wall VDW interaction domain. The distribution of density along the length of the adhesive is shown in Fig. 10 where it is apparent that the density distribution is more oscillatory for the 2 nm thick adhesive. The oscillatory density reduces significantly in the core where the wall interaction is out-of-range, and it is evident from Fig. 10 that the length of the flatter core increases with increase in thickness. Note that the core is the least dense zone of the adhesive and, reasonably, the weakest part of the adhesive structure. In the nanoscale range, the volume of the *EVZ* is significant compared with to the total volume of the adhesive which, in turn, causes structural changes in the adhesive. Such changes can be measured from the variation of average radius of gyration ($\langle R_g \rangle$) or end-to-end distance ($\langle R_{ee} \rangle$) of the confined polymer with respect to its bulk counterpart [21]. It is known that any increase in $\langle R_g \rangle$ or $\langle R_{ee} \rangle$ also qualitatively implies improved mechanical properties of polymers [14].

4.3 Effect of Bondline Thickness on the Joint Strength

From practical interests, the thickness effect of adhesive is important when joints fail in a cohesive manner. It is already observed for tensile loading that cohesive failure of joints occurs when $u_{wa} \geq 1.0 u_{wa}^0$, where cavitation in the polymer is the failure mechanism. By monitoring the sequence of snapshots (not shown here) from the beginning of deformation, it is observed that cavitation always nucleates from the core and then expands in three dimensions. We can observe from Fig. 3 that as long as the deformation leads to cohesive failure, the strength of the adhesive increases as the thickness of the adhesive decreases. Basu and Kulmi [4] reported that the tensile strength of a joint is enhanced by decreasing the adhesive thickness only when the failure mode is purely cohesive. They did not include any other mode of loading in their study. We have included shear and combined loading in

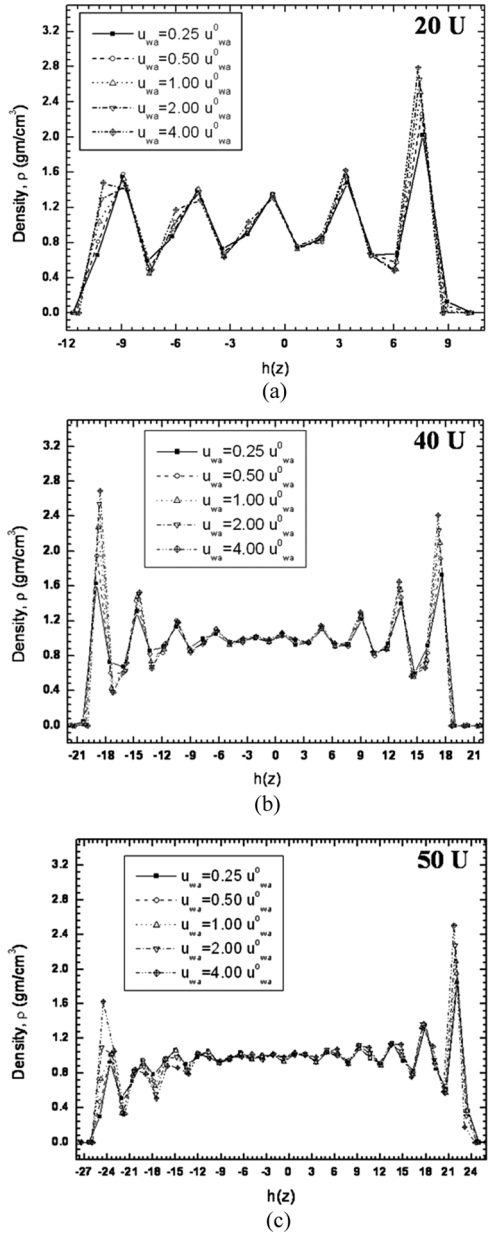

FIGURE 10 Segmental density distribution of (a) 2 nm, (b) 4 nm, and (c) 5 nm adhesives.

this study and found from the response in shear (Fig. 4) that even though the mode of failure is not purely cohesive ($u_{wa} > 2.0u^0_{wa}$), the thickness effect still exists. For combined loading (Fig. 5), cohesive failure is hard to achieve, and the thickness effect is less pronounced. We can view the effect of adhesive thickness on joint strength from two perspectives: density of the adhesive and configurational change in polymer due to confinement [4,21]. It is evident from Fig. 10 that, for $u_{wa} = 4.0u^0_{wa}$, near-wall ρ_{max} of adhesive varied from 2.5 to 2.8 g/cm^3 as adhesive thickness is reduced from 5 to 2 nm. The core density remains the same for all joints. This indicates that the overall density in the two *EVZ* is higher for thinner adhesives which, in turn, indicates that the stiffness of adhesives in this zone would be higher. When joints are loaded in tension, they first yield due to the nucleation of cavitation in the core. At this stage, the joint reaches its peak stress. The magnitude of stress then gradually reduces as deformation continues "plastically". In other words, the magnitude of the peak stress depends on the growth and expansion rate of cavitation in the core. The presence of a higher density polymer layer at the top and bottom of the adhesives resists the expansion of cavitation and, therefore, implies a higher load carrying capacity of joints. It can be seen from Fig. 10 that the width of the low-density core increases with increase in thickness, indicating that the expansion of cavitation is least resisted when thickness is increased and *vice-versa.*

Apart from density variation, it is found that the confinement of polymer chains also leads to significant increase in the failure strength, especially in tensile loading. It is reported [4] that reducing thickness to a value comparable with $\langle R_{ee} \rangle$ switches the failure mode from cohesive-adhesive failure to purely cohesive failure and, thus, improves the overall yield strength significantly. In our simulation, we found that $\langle R_{ee} \rangle$ varies from 17.89 to 20.62 Å as thickness decreases from 5 to 2 nm. Our finding is consistent with experimental observations of chain confinements and their relation to chain configurations [21]. As pointed out earlier that increase in $\langle R_{ee} \rangle$ affects polymer properties, we believe that this is possibly another reason why reduction of adhesive thickness increases the overall failure strength of joints [4].

It can be recalled that, unlike other researchers [8–18], Chai [11] found a reverse trend in the thickness effect on joint properties in the sense that the joint started to show improved toughness as adhesive thickness was reduced to 0.033 mm or smaller. Even though Chai's [11] joints were three to four orders of magnitude thicker than what we studied here, our results qualitatively confirm his findings.

5. CONCLUSIONS

In this work, we have studied the effect of adhesive thickness and the quality of the interface on the deformation and failure of glassy polymer adhesives using molecular dynamics simulations. The mechanical responses of joints under tensile, shear, and combined tensile-shear loads were considered. The following conclusions are drawn from this study.

1. The overall density of polymers significantly increases when they are confined between adherends at nanoscale separations. The increased density is attributed to the VDW attraction between adherend walls and polymer core which transforms the regular amorphous polymer to densely packed layers near the adherend wall. Adhesives are found to be more than twice as dense in the layered region. The effective thickness of this layer region depends on the range of VDW interaction which appears to be $\sim$1 nm.
2. The failure mode of adhesive joints primarily depends on the strength of adherend-adhesive interfacial adhesion. In the case of a weaker interfacial adhesion, joints always fail at the interface. Cohesive failure is possible in the presence of stronger interfaces where deformation of adhesive occurs through cavitation under tensile loads and through bulk shear under shear loading. A relatively strong interface is required to guarantee pure shear loading compared with pure tension; otherwise, all failures will be interfacial. It is also observed that bulk shear is hard to realize under the mixed-mode condition.
3. In the case of cohesive failure, yielding of joints also depends on interfacial strength. This is a special feature of nano-adhesives, as macroscopically cohesive failure is independent of the interface strength because *EVZ* is negligible in macroscopic adhesive joints. This counterintuitive behavior is attributed to the change in adhesive density with change in interface strength that ultimately governs the failure strength.
4. Failure strength of joints in tension or shear considerably increases as adhesive thickness is reduced. The increase in strength is due to increase in density and $\langle R_{ee} \rangle$ of polymer chains.
5. The current study qualitatively reveals some insight on the effect of bondline thickness on the failure of nanoscale adhesives. We found that the intermolecular forces between the adherend and the adhesive primarily dictate the failure strength of the joint. It is the relative proportion of "active zone" compared with bondline

thickness that imparts the thickness effect. Since the non-bonded forces are very short-ranged (~1 nm), we expect that joint properties will be independent of thickness for thicker joints. Some multiscale modeling will be suitable to explore the thickness effect with micron or sub micron scale adhesives.

We would like to caution the readers not to interpret our results as an explanation for experimental trends [8–10] discussed earlier. It is apparent that the length scale of our MD simulation and the length scale of the cited references are several orders of magnitude different. The purpose of the current MD simulations were two fold–whether there exists any thickness effect in the nanoscale, and whether we can provide any "qualitative" explanation for such interesting trends in adhesive joints.

ACKNOWLEDGMENT

This work was supported by a National Science Foundation Grant No. HRD-976871.

REFERENCES

[1] Pocius, A. V., *Adhesion and Adhesives Technology*, (Hanser Gardner Publications Inc., Munich, 2002), Ch. 1, pp. 5–11.
[2] Sarwar, F., Hutt, D. A., and Whalley, D. C., *Proceedings of POLYTRONIC, Second International IEEE Conference on Polymers and Adhesives in Microelectronics and Photonics*, (2002), pp. 22–28.
[3] Jorg, R. and Robbins, M. O., *J. Adh. Sci. Tech.* **17**, 369–381 (2003).
[4] Basu, S. and Kulmi, U., *Model. Simul. Mater. Sci. Eng.* **14**, 1071–1093 (2006).
[5] Da Silva, L. F. M., Rodrigues, T. N. S. S., Figueiredo, M. A. V., de Moura M. F. S. F., and Chousal J. A. G., J. *Adhesion* **82**, 1091–1115 (2006).
[6] Adams, D. and Grant, L. D. R., *Proceedings of 16th Annual Meeting of Adhesion Society*, (1993), pp. 91–93.
[7] Objois A., Gilbert, Y., and Fargette, B., *J. Adhesion* **70**, 13–32 (1999).
[8] Bascom W. D., Cottington R. L., Jones R. L., and Peyser P., *J. Appl. Polym. Sci.* **19**, 2545–2562 (1976).
[9] Kinloch A. J. and Shaw S. J., *J. Adhesion* **12**, 59–77 (1981).
[10] Lee D. B., Ikeda T., Miyazaki N., and Choi N. S., *J. Eng. Mater.-T ASME* **126**, 14–18 (2004).
[11] Chai H. *Composite Materials: Testing and Design*, *Seventh Conference ASTM STP 893*, J. M. Whitney (Ed.) (American Society for Testing and Materials, Philadelphia, PA, USA 1986), pp. 209–231.
[12] Binder, K., *Monte Carlo and Molecular Dynamics Simulations in Polymer Science*, (Oxford University Press, New York, 1995).
[13] Allen, M. P. and Tildesley, D. J., *Computer Simulations of Liquids*, (Oxford University Press, New York, 1987).

[14] Sperling, L. H., *Introduction to Physical Polymer Science*, (John Wiley & Sons, Inc., New Jersey, 2006).
[15] Kremer, K. and Grest, G. S., *J. Chem. Phys.* **92**, 5057–5086 (1990).
[16] Jorgensen, W. L., Madura, J. D., and Swensen, C. J., J. Am. Chem. Soc. **106**, 638–646 (1984).
[17] Smith, W. and Rodger, P. M., *Internet Source:http://www.ccp5.ac.uk/infoweb/wsmith22/wsmith22.pdf(2002)*. Accessed May 7, 2008
[18] Smith, W. and Forester, T. R., *DLPOLY-2.14 manual. Internet Source:http://www.cse.scitech.ac.uk/ccg/software/DL_POLY*. Accessed May 7, 2008.
[19] Smith, W. and Forester, T. R., *J. Mol Grap* **14**, 136–141 (1996).
[20] Frankland, S. J. V., Caglar, A., Brenner, D. W., and Griebel, M., *J. Phys. Chem B* **106**(12), 3046–3048 (2002).
[21] Kraus, J., Mauller-Buschbaum, P., Kuhlmann, T., Schubert D. W., and Stamm, M., *Europhys. Lett.* **49**, 210–216 (2000).